

**Periodically forced ensemble of nonlinearly coupled oscillators: From partial to full synchrony**Yernur Baibolatov,<sup>1,2</sup> Michael Rosenblum,<sup>1</sup> Zeinulla Zh. Zhanabaev,<sup>2</sup> Meyramgul Kyzgarina,<sup>2</sup> and Arkady Pikovsky<sup>1</sup><sup>1</sup>*Department of Physics and Astronomy, University of Potsdam, Karl-Liebknecht-Str. 24/25, D-14476 Potsdam-Golm, Germany*<sup>2</sup>*Department of Physics, Al-Farabi Kazakh National University, Tole bi Str. 96, 050012 Almaty, Kazakhstan*

(Received 29 July 2009; published 22 October 2009)

We analyze the dynamics of a periodically forced oscillator ensemble with global nonlinear coupling. Without forcing, the system exhibits complicated collective dynamics, even for the simplest case of identical phase oscillators: due to nonlinearity, the synchronous state becomes unstable for certain values of the coupling parameter, and the system settles at the border between synchrony and asynchrony, what can be denoted as partial synchrony. We find that an external common forcing can result in two synchronous states: (i) a weak forcing entrains only the mean field, whereas the individual oscillators remain unlocked to the force and, correspondingly, to the mean field; (ii) a strong forcing fully synchronizes the system, making the phases of all oscillators identical. Analytical results are confirmed by numerics.

DOI: [10.1103/PhysRevE.80.046211](https://doi.org/10.1103/PhysRevE.80.046211)

PACS number(s): 05.45.Xt

**I. INTRODUCTION**

Ensembles of globally, or all-to-all, coupled oscillators serve as models for many physical, chemical, biological, etc., systems allowing one to describe diverse natural phenomena as synchronous blinking of fireflies, pedestrian synchrony on the millennium bridge, emergence of brain rhythms, just to mention a few [1–7]. The main effect is the self-synchronization and the appearance of a collective mode in an ensemble of generally nonidentical elements—the problem relevant for Josephson junction and laser arrays [8,9], electrochemical reactions [10], neuronal dynamics [11], human social behavior [12–14], etc. This collective mode arises due to an adjustment of frequencies and phases of at least some group of the elements; the larger is this synchronized group, the larger the amplitude of the collective mode.

An ensemble, exhibiting the collective mode, can be considered as a macroscopic oscillator. A natural idea is to analyze the response of this oscillator to an external perturbation or to a coupling to another macroscopic oscillator (ensemble). This study is relevant, e.g., for modeling of neuronal rhythms in the case when an ensemble of interacting neurons is influenced by rhythms from other brain regions [15–17]. In particular, one can analyze a collective phase resetting by pulsatile stimuli [18–20], entrainment of the collective mode by external forcing [21–23], mutual synchronization of two ensembles [24,25], suppression or enhancement of the collective mode by a feedback [26,27], etc. In the first approximation, the macroscopic oscillator behaves like a usual limit cycle oscillator and the description of the dynamics in this approximation can be obtained by means of a model equation for the collective mode, incorporating the terms responsible for forcing, coupling [24], or feedback [26,27], respectively. However, there are interesting effects which go beyond this simplistic description. For example, the coupling between populations of identical units can destroy synchrony in one of the populations and cause a *partially synchronous chimera state* [28], when the phases of individual units are not adjusted, but the collective mode exist, though its amplitude is reduced with respect to that in the synchronous state. Another effect is the appearance of

synchronous subgroups with different frequencies in a harmonically forced ensemble of nonidentical elements [21].

In the present paper we study the effects of periodic forcing on an oscillator ensemble that by itself exhibits complex dynamics even in the simplest setup of identical units. Namely, we consider ensembles with *global nonlinear coupling* (see [29,30] and a detailed discussion below). Due to nonlinearity in the coupling, the completely synchronous state loses its stability upon increase in the coupling strength, whereas the completely asynchronous state remains unstable as well. As a result, for a sufficiently large coupling, such ensembles demonstrate an intermediate state of partial synchrony, when the phases of oscillators are nonuniformly distributed between 0 and  $2\pi$ . Especially interesting is the regime of self-organized quasiperiodicity, when the frequency of the collective mode differs from the frequency of individual oscillators. Here we demonstrate that nonlinearly coupled ensembles, subject to external forcing, exhibit nontrivial synchronization properties. We show that a harmonic external force can destroy partial and induce full synchrony; however, it is also possible that the forcing entrains only the collective mode but not individual oscillators.

The paper is organized as follows. In the next section we describe the basic model of the ensemble of phase oscillators with global nonlinear coupling. In Sec. III we use the Watanabe-Strogatz theory to derive the equation for the collective dynamics of the driven system. In Secs. IV and V we analyze regimes of full synchrony and of mean-field locking, respectively. In Sec. VI we summarize and discuss our results.

**II. BASIC PHASE MODEL****A. Kuramoto-Sakaguchi model**

A paradigmatic model for the description of the dynamics of large ensembles of weakly interacting units is the Kuramoto model [1,2] of each-to-each, or globally coupled phase oscillators. The model reads

$$\dot{\phi}_k = \omega_k + \frac{\varepsilon}{N} \sum_{j=1}^N \sin(\phi_j - \phi_k + \beta), \quad (1)$$

where  $\phi_k$  and  $\omega_k$  are the phase and the natural frequency of the  $k$ -th oscillator,  $N$  is the number of oscillators in the ensemble,  $\varepsilon$  is the strength of the interaction within each pair of oscillators. Generally, the model can also include a constant phase shift  $\beta$ ; this case is also called the Kuramoto-Sakaguchi model [31]. It is convenient to rewrite Eq. (1) as

$$\dot{\phi}_k = \omega_k + \frac{\varepsilon}{N} \sum_{j=1}^N \text{Im}[e^{i\phi_j} e^{i(-\phi_k + \beta)}] = \omega_k + \text{Im}(\varepsilon e^{i\beta} Z e^{-i\phi_k}), \quad (2)$$

where  $Z$  is the complex Kuramoto order parameter, or the mean field

$$Z = r e^{i\Theta} = N^{-1} \sum_{k=1}^N e^{i\phi_k}.$$

The mean-field amplitude, or the real order parameter  $r$ , varies from zero in the absence of synchrony to one, if all elements have identical phases.

### B. Generalization to nonlinear coupling

Recently, the Kuramoto model has been generalized [29,30] to cover the case of coupled ensembles with nonlinear interaction between oscillators. ‘‘Nonlinear’’ in this context means that the effect of the force on an oscillator qualitatively depends on the amplitude of the forcing, e.g., a weak force tends to induce in-phase synchrony, whereas a stronger force tends to synchronize the oscillator in antiphase. In case of a globally coupled ensemble, nonlinear interaction means a dependence of the form of the coupling function on the mean-field amplitude  $r$ . In other words, with a variation in a bifurcation parameter, the interaction can change from an attractive one to a repulsive one. The generalized model reads

$$\dot{\phi}_k = \omega_k(r, \varepsilon) + \text{Im}[\varepsilon A(r, \varepsilon) e^{i\beta(r, \varepsilon)} Z e^{-i\phi_k}], \quad (3)$$

where  $\omega_k(r, \varepsilon)$ ,  $A(r, \varepsilon)$ , and  $\beta(r, \varepsilon)$  are some functions of the amplitude of the mean field  $r=|Z|$ . The model can be treated analytically for the case of identical oscillators  $\omega_k=\omega$ , see [29,30]. It is easy to show that the fully synchronous cluster state ( $\phi_1=\phi_2=\dots=\phi_N=\Theta$ ,  $r=1$ ) is stable if  $A(r, \varepsilon)\cos\beta(r, \varepsilon)>0$ . When either the amplitude function  $A$  or the phase function  $\cos\beta$  changes its sign upon an increase in the coupling strength  $\varepsilon$ , the synchronous cluster dissolves and a partial synchrony arises.

If the loss of synchrony occurs via zero crossing of the  $A$  function, whereas  $\cos\beta$  remains positive, a regime appears where the oscillator phases scatter on the circle, but their distribution is not uniform. It means that the mean-field amplitude is  $0<r<1$ . The frequency of the mean field equals that of oscillators,  $\Omega=\langle\dot{\Theta}\rangle=\omega_{osc}=\langle\dot{\phi}\rangle$ . The appearance of this partially synchronous state can be easily understood qualitatively (for a quantitative analysis see [30]). Assume

for definiteness that  $A$  is a monotonically decreasing function of  $\varepsilon$  and  $r$  and is positive for small  $\varepsilon$  and  $r=1$ , so that the completely asynchronous state ( $r=0$ ) is unstable, and  $A(1, \varepsilon_b)=0$  for some critical value  $\varepsilon_b$ . Then the fully synchronous state is stable for  $\varepsilon<\varepsilon_b$  and unstable for  $\varepsilon>\varepsilon_b$ . Hence, for  $\varepsilon>\varepsilon_b$  the oscillators tend to desynchronize, but they cannot desynchronize completely, because with the decrease of  $r$  the function  $A$  becomes positive again, what means that the interaction becomes attractive, so that the oscillators again tend to synchronize. As a result of this counterplay the system settles at the border of stability so that  $A(r, \varepsilon)=0$ ; this equation determines the mean-field amplitude  $r$  as a function of  $\varepsilon$ . The described state is called the self-organized bunch state (SOB) [30].

The most interesting effect is observed if the function  $\cos\beta$  becomes zero. In this regime the oscillators are not locked to the mean field they produce, so that in this state the oscillators and the mean field have different frequencies,  $\omega_{osc} \neq \dot{\Theta}$ . These frequencies are smooth functions of the coupling strength  $\varepsilon$ , what means that generally they are incommensurate. We denote this dynamics as self-organized quasi-periodicity (SOQ). This state is also characterized by a nonuniform scattering of phases, and, hence, by the mean-field amplitude in the range  $0<r<1$ ; it emerges from the fully synchronous state with  $r=1$  via a desynchronization transition when the function  $\cos\beta$  crosses zero upon increase in the coupling strength  $\varepsilon$ . Again, the peculiar feature of the state is that with the variation in the coupling strength beyond a critical value  $\varepsilon_q$ , the system always stays exactly on the border of stability, when full synchrony is lost and partial synchrony sets in. This border is determined by the condition  $\beta(1, \varepsilon_q)=\pm\pi/2$ , and for  $\varepsilon>\varepsilon_q$  the system is organized in a way that it stays at this critical state, so that  $\beta(r, \varepsilon)=\pm\pi/2$ ; the latter expression provides the dependence  $r(\varepsilon)$ . Hence, the mean-field amplitude also smoothly depends on  $\varepsilon$ . The quantitative analysis of SOQ dynamics can be found in [29,30].

### C. Forced ensembles

In this paper we analyze the dynamics of an ensemble with global nonlinear coupling, described by Eq. (3), under an external periodic forcing. This study is relevant, e.g., for modeling of neuronal rhythms in case when an ensemble of interacting neurons is influenced by rhythms from other brain regions. On the other hand, this study is a first step to consideration of an interesting problem of two interacting nonlinearly coupled ensembles. In our analysis we restrict ourselves to the case of identical oscillators, when the model (3) of the autonomous ensemble can be treated analytically [29,30], and introduce a harmonic forcing  $\mu e^{i\bar{\nu}t}$ , where  $\mu$  and  $\bar{\nu}$  are the amplitude and the frequency of the external force. The model reads

$$\dot{\phi}_k = \omega(r, \varepsilon) + \text{Im}[\varepsilon A(r, \varepsilon) e^{i\beta(r, \varepsilon)} Z e^{-i\phi_k} + \mu e^{i(\bar{\nu}t - \phi_k)}]. \quad (4)$$

Next, we take  $\omega(\varepsilon, r)=\omega=\text{const}$  and make a transformation to a frame, rotating with the frequency  $\omega$ . The phases of oscillators and of the mean field are then transformed to slow

phases as  $\phi_k \rightarrow \phi_k + \omega t$ ,  $\Theta \rightarrow \Theta + \omega t$  and the equations in the rotating frame are:

$$\dot{\phi}_k = \text{Im}[He^{-i\phi_k}], \quad (5)$$

$$H = \varepsilon A(r, \varepsilon) e^{i\beta(r, \varepsilon)} r e^{i\Theta} + \mu e^{i\nu t}, \quad (6)$$

where  $\nu = \tilde{\nu} - \omega$  is the frequency mismatch. Here we have also introduced the *complex effective force*  $H$ , acting on individual oscillators.

In the following analysis we concentrate separately on the effect of the amplitude function  $A(\varepsilon, r)$  and of the phase shift function  $\beta(\varepsilon, r)$ . In other words, we concentrate on two cases when the unforced system is partially synchronous either in the SOB or in the SOQ state. We demonstrate and analyze two different synchronous regimes: (i) the external force entrains only the mean field, but not individual oscillators and (ii) the regime of full synchrony, when the force entrains all oscillators and, hence, destroys the SOQ/SOB regime.

### III. WATANABE-STROGATZ EQUATIONS FOR THE FORCED OSCILLATOR ENSEMBLE

A complete analysis of the model (5) and (6) can be performed by means of the Watanabe-Strogatz (WS) theory [32,33]. Their main result is that for any time-dependent function  $H(t)$  the  $N$ -dimensional system of identical oscillators (5) can be reduced to a three-dimensional system for global variables  $\rho$ ,  $\Phi$ ,  $\Psi$  [40]:

$$\frac{d\rho}{dt} = \frac{1 - \rho^2}{2} \text{Re}(He^{-i\Phi}), \quad (7)$$

$$\frac{d\Phi}{dt} = \frac{1 + \rho^2}{2\rho} \text{Im}(He^{-i\Phi}), \quad (8)$$

$$\frac{d\Psi}{dt} = \frac{1 - \rho^2}{2\rho} \text{Im}(He^{-i\Phi}). \quad (9)$$

Here  $0 \leq \rho \leq 1$  is the global amplitude and  $\Phi$ ,  $\Psi$  are global phases; their meaning is discussed below. The original phase variables can be reconstructed from the WS variables by means of the time-dependent transformation

$$\phi_k = \Phi(t) + 2 \arctan \left[ \frac{1 - \rho(t)}{1 + \rho(t)} \tan \left( \frac{\psi_k - \Psi(t)}{2} \right) \right]. \quad (10)$$

Here  $\psi_k$  are  $N$  constants of motion, which should obey three constraints, otherwise the transformation is overdetermined; this is discussed in detail in [33]. It is convenient to choose two constraints as follows:

$$\sum_{k=1}^N \cos \psi_k = 0, \quad \sum_{k=1}^N \sin \psi_k = 0. \quad (11)$$

The third condition on  $\psi_k$  is somehow arbitrary, it only fixes the common shift of  $\psi_k$  with respect to  $\Psi$ . It can be taken, e.g., as  $\sum_k \psi_k = 0$  (this implies that constants are defined in the  $[-\pi, \pi]$  interval) [33]. Another convenient choice is  $\sum \cos(2\psi_k) = 0$ . These conditions allow one to determine un-

ambiguously the variables  $\rho(0)$ ,  $\Psi(0)$ ,  $\Phi(0)$ , and constants  $\psi_k$  from the initial conditions  $\phi_k(0)$ , except for the case when initial state contains too large clusters (see [33] for details).

Our next goal is to relate the WS variables to the Kuramoto mean field  $Z = r e^{i\Theta}$ . This can be done by rewriting the transformation Eq. (10) in the following form [34,35]

$$e^{i\phi_k} = e^{i\Phi(t)} \frac{\rho(t) + e^{i[\psi_k - \Psi(t)]}}{1 + \rho(t) e^{i[\psi_k - \Psi(t)]}}. \quad (12)$$

With the help of this equation the combination of two WS variables, namely,  $\rho e^{i\Phi}$ , can be related to  $Z$  as follows [34]:

$$r e^{i\Theta} = N^{-1} \sum_{k=1}^N e^{i\phi_k} = \rho e^{i\Phi} \gamma(\rho, \Psi), \quad (13)$$

where

$$\gamma(\rho, \Psi) = N^{-1} \sum_{k=1}^N \frac{1 + \rho^{-1} e^{i(\psi_k - \Psi)}}{1 + \rho e^{i(\psi_k - \Psi)}}. \quad (14)$$

The obtained relation helps to understand the physical meaning of the WS variables. The amplitude variable  $\rho$  is roughly proportional to the mean-field amplitude  $r$ . Indeed, if  $\rho=0$ , then from Eq. (12) with account of Eq. (11), we obtain  $r=0$ . From Eqs. (13) and (14) obviously follows that  $\rho=1$  yields  $r=1$ . For intermediate values  $0 < \rho < 1$  the relation between  $\rho$  and  $r$  generally depends also on  $\Psi$ . The phase variable  $\Phi$  characterizes the position of the maximum in the distribution of phases and is therefore close to the phase of the mean field  $\Theta$ . They coincide for  $\rho=r=1$ ; for  $0 < \rho < 1$ ,  $\Phi$  is shifted with respect to  $\Theta$  by an angle that depends on  $\rho$ ,  $\Psi$ . Finally, the second global phase variable  $\Psi$  determines the shift of individual oscillators with respect to  $\Phi$ . As it follows from Eq. (10),  $\phi_k$  grows by  $2\pi$  when  $\Psi$  decreases by  $2\pi$ . Hence, for the time averaged phase growth we obtain  $\langle \dot{\phi}_k \rangle = \omega_{osc} = \langle \dot{\Phi} \rangle - \langle \dot{\Psi} \rangle$ . For the following it is useful to write, using Eqs. (8) and (9), the expression for the oscillator frequency as:

$$\omega_{osc} = \left\langle \dot{\Psi} \frac{2\rho^2}{1 + \rho^2} \right\rangle. \quad (15)$$

We emphasize now an important case when WS Eqs. (7)–(9) simplify. As it was shown in [34], for large  $N$  and uniform distribution of constants of motion  $\psi_k$ , factor  $\gamma$  in Eq. (13) equals one, and, hence,  $\rho=r$ ,  $\Phi=\Theta$ . This also means that  $H$  depends on  $\rho$  and  $\Phi$  and does not depend on  $\Psi$ . As a result, from three Eqs. (7)–(9) for Watanabe-Strogatz variables we obtain two equations for the amplitude and phase of the Kuramoto mean field  $r$ ,  $\Theta$ :

$$\frac{dr}{dt} = \frac{1 - r^2}{2} \text{Re}(He^{-i\Theta}), \quad (16)$$

$$\frac{d\Theta}{dt} = \frac{1 + r^2}{2r} \text{Im}(He^{-i\Theta}). \quad (17)$$

An analysis of these equations, performed in the following sections, yields a description of synchronous states in the forced ensemble; there we also present numerical results for

the case of nonuniformly distributed  $\psi_k$ . We note that the case of uniformly distributed constants of motion, i.e.,  $\gamma=1$ , corresponds to the recent Ott-Antonsen ansatz [23] (this correspondence was shown in [34]). Noteworthy, this is not just a solvable, but also the mostly interesting case, because for a continuous distribution of oscillator frequencies the corresponding solutions are the only attractors [36]. However, we emphasize that Eqs. (16) and (17) are also valid for an arbitrary distribution of constants  $\psi_k$  in the particular case of full synchrony  $\rho=1$ , since  $\gamma(1, \Psi)=1$ .

For the further analysis of synchronous states it is convenient to present the phase shift  $\delta=\nu t-\Theta$  between the external force and the mean field and, with account of Eq. (6), to rewrite Eqs. (16) and (17) as:

$$\dot{r} = \frac{1-r^2}{2} [\varepsilon A(r, \varepsilon) r \cos \beta(r, \varepsilon) + \mu \cos \delta], \quad (18)$$

$$\dot{\delta} = \nu - \frac{1+r^2}{2r} [\varepsilon A(r, \varepsilon) r \sin \beta(r, \varepsilon) + \mu \sin \delta]. \quad (19)$$

A solution of these equations with bounded  $\delta$  describes synchronization of the ensemble by the external force. Below we consider different cases, starting with the full synchrony in Sec. IV and proceeding to the mean-field locking in Sec. V. Our starting point is the unforced system (18) and (19) in a state of partial synchrony with  $0 < r < 1$ , resulting from the condition  $A(r, \varepsilon) \cos \beta(r, \varepsilon) = 0$ . We analyze the effects of the forcing taking its amplitude  $\mu$  and frequency  $\nu$  as main parameters.

#### IV. FULL SYNCHRONIZATION

In this section we analyze the case when the external force entrains all oscillators in the initially partially synchronized ensemble and imposes the regime of full synchrony (FS),  $\phi_1 = \dots = \phi_N = \Theta$ ,  $r=1$ . Then Eq. (19) yields

$$\dot{\delta} = \nu - \varepsilon A(1, \varepsilon) \sin \beta(1, \varepsilon) - \mu \sin \delta. \quad (20)$$

This is a first-order equation for  $\delta$ , it can have fixed points and running solutions. The former correspond to fully synchronous state. As follows from Eq. (18), such a solution is stable if

$$\varepsilon A(1, \varepsilon) \cos \beta(1, \varepsilon) + \mu \cos \delta > 0, \quad (21)$$

or

$$\mu \cos \delta > |\varepsilon A(1, \varepsilon) \cos \beta(1, \varepsilon)|. \quad (22)$$

[We remind that the unforced ensemble is in the state of partial synchrony, what implies that  $\varepsilon A(1, \varepsilon) \cos \beta(1, \varepsilon) < 0$ .] This means that the fully synchronous regime exists only if the forcing is sufficiently strong,  $\mu > \mu_c$ , where

$$\mu_c = |\varepsilon A(1, \varepsilon) \cos \beta(1, \varepsilon)|. \quad (23)$$

Thus, for the border of the domain of FS we have

$$\mu \sin \delta = \nu - \varepsilon A(1, \varepsilon) \sin \beta(1, \varepsilon), \quad (24)$$

$$\mu \cos \delta = \varepsilon |A(1, \varepsilon) \cos \beta(1, \varepsilon)| = \mu_c. \quad (25)$$

Excluding  $\delta$  we obtain the equation for the border of the synchronization region (tongue)

$$[\nu - \varepsilon A(1, \varepsilon) \sin \beta(1, \varepsilon)]^2 + [\varepsilon A(1, \varepsilon) \cos \beta(1, \varepsilon)]^2 = \mu^2. \quad (26)$$

The variation in the phase shift  $\delta$  between the external force and the mean field across the tongue, i.e., for fixed  $\mu$ , is determined by Eq. (24). The range of this variation follows from Eq. (25), so that  $-\delta_{\max} \leq \delta \leq \delta_{\max}$ , where  $\delta_{\max} = \arccos(\mu_c/\mu)$ ; for large  $\mu$ ,  $\delta_{\max} \rightarrow \pi/2$ . For comparison, recall that synchronization regions for one driven oscillator or for a driven ensemble of identical linearly coupled phase oscillators are of a triangular shape, the synchronization threshold is zero, and the variation in the phase shift across the region is  $-\pi/2 \leq \delta \leq \pi/2$ .

Below we analyze the fully synchronous solution for two particular cases, when the partial synchrony in the unforced system arises either due to the amplitude function  $A(r, \varepsilon)$  or due to the phase function  $\beta(r, \varepsilon)$ . These cases correspond to the SOB and SOQ states in the unforced system, respectively.

#### A. SOB state in the unforced system

For definiteness, we consider the model (5) and (6) with  $\varepsilon A(r, \varepsilon)$  monotonically decreasing with the mean-field amplitude  $r$  and the coupling  $\varepsilon$ . Suppose that  $A(r, \varepsilon)$  vanishes for some critical coupling  $\varepsilon_b$ , determined from the condition  $A(1, \varepsilon_b) = 0$ . Suppose also that  $|\beta(r, \varepsilon)| = \text{const} < \pi/2$ . Then for  $\varepsilon > \varepsilon_b$  the synchronous solution of the unforced system,  $\mu=0$ , becomes unstable due to the amplitude function and we observe an SOB state. For  $\varepsilon > \varepsilon_b$  we have  $A(1, \varepsilon) < 0$  and Eq. (23) yields

$$\mu_c = |\varepsilon A(1, \varepsilon)| \cos \beta(1, \varepsilon). \quad (27)$$

Using  $\varepsilon A(1, \varepsilon) \sin \beta(1, \varepsilon) = -\sqrt{[\varepsilon A(1, \varepsilon)]^2 - \mu_c^2}$ , we obtain from Eq. (26) the equation for the border of the tongue:

$$\nu_{l,r} = -\sqrt{[\varepsilon A(1, \varepsilon)]^2 - \mu_c^2} \pm \sqrt{\mu^2 - \mu_c^2}. \quad (28)$$

Here indices  $l$  and  $r$  denote the left and the right border of the tongue, respectively. The tip of the tongue has coordinates  $[-\varepsilon |A(1, \varepsilon)| \sin \beta(1, \varepsilon), \varepsilon |A(1, \varepsilon)| \cos \beta(1, \varepsilon)]$ , so that for a fixed  $\varepsilon$  it stays on a circle with radius  $\varepsilon |A(1, \varepsilon)|$ , centered at the origin (Fig. 1). Note, that the tongue is parabolic for  $\mu - \mu_c \ll \mu_c$ . Note also that for  $\beta(1, \varepsilon) \rightarrow \pm \pi/2$  the synchronization threshold vanishes and the tongue becomes triangular,  $\nu_{l,r} = -\varepsilon |A(1, \varepsilon)| \pm \mu$ .

We illustrate the theory by simulating an ensemble of 1000 oscillators for  $\beta = \pi/4$  and  $A = 1 - \varepsilon r^2$ . For each point in the parameter plane  $\nu, \mu$  we run the simulation with two sets of initial conditions: nearly uniform and nearly identical [41]. These numerical results are presented in Fig. 2; they demonstrate that numerically obtained domain of the full synchrony has a good correspondence with the theory. In addition, we find that the system is multistable: in a certain region the nearly identical initial conditions lead to full syn-

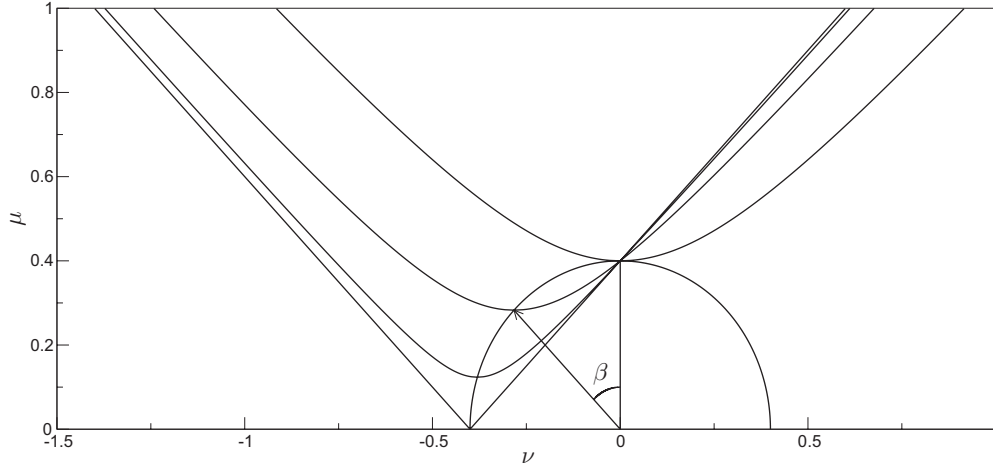


FIG. 1. Regions (tongues) of full synchrony for the harmonically forced ensemble with global nonlinear coupling [see Eqs. (5) and (6)] with  $\beta = \text{const}$  and  $A = 1 - \varepsilon r^2$ . With a variation in  $\beta$ , the tip of the tongue moves along a circle with radius  $\varepsilon - 1$ . The tongues are plotted for  $\beta = 0, \beta = 0.25\pi, \beta = 0.4\pi$ , and  $\beta = 0.5\pi$ ; the value of coupling is  $\varepsilon = 1.4$ .

chrony, whereas the nearly uniform initial conditions result in an asynchronous state.

**B. SOQ state in an unforced system**

Now we consider the model (5) and (6) with the amplitude function  $A$ , which has no roots and is positive, and the phase-shift function  $\beta(r, \varepsilon)$ , that monotonically increases with the mean-field amplitude  $r$  and the coupling  $\varepsilon$ . We recall that for  $\varepsilon > \varepsilon_q$ , where  $\varepsilon_q$  is determined from the condi-

tion  $\beta(1, \varepsilon_q) = \pi/2$ , the system exhibits SOQ. Then, for  $\varepsilon > \varepsilon_q$  we have  $\beta(1, \varepsilon) > \pi/2$  and Eq. (23) yields for the critical forcing amplitude

$$\mu_c = \varepsilon A(1, \varepsilon) |\cos \beta(1, \varepsilon)|.$$

Then from Eq. (26) we find the border of the tongue:

$$\nu_{l,r} = \varepsilon A(1, \varepsilon) \sin \beta(1, \varepsilon) \pm \sqrt{\mu^2 - \mu_c^2}. \tag{29}$$

Again, like in the previous example, the region is not triangular but parabolic for  $\mu - \mu_c \ll \mu_c$ . The tip of the tongue has coordinates  $[\varepsilon A(1, \varepsilon) \sin \beta(1, \varepsilon), \varepsilon A(1, \varepsilon) |\cos \beta(1, \varepsilon)|]$ . Varying  $\varepsilon$  we see that the tip of the tongue moves along a spiral. For an illustration we take the model with  $A = 1$  and  $\beta = \beta_0 + \varepsilon^2 r^2$  and assume that the coupling  $\varepsilon$  is not too strong so that  $\cos \beta(1, \varepsilon)$  remains negative,  $\beta(1, \varepsilon) \leq 3\pi/2$ , i.e., the condition for SOQ dynamics in an unforced system holds. It means that the coupling satisfies  $\varepsilon_q \leq \varepsilon \leq \sqrt{\pi + \varepsilon_q^2}$ . The theory is illustrated in Fig. 3 and the numerical results for 1000 oscillators,  $\varepsilon = 0.4$ , and  $\beta_0 = 0.475\pi$  are shown in Fig. 4. One can see that the border of the full synchronization domain determined according to Eq. (29) corresponds to the numerics. Again, we find multistability with respect to initial conditions: for certain parameter values a fully synchronous solution coexists with an asynchronous one.

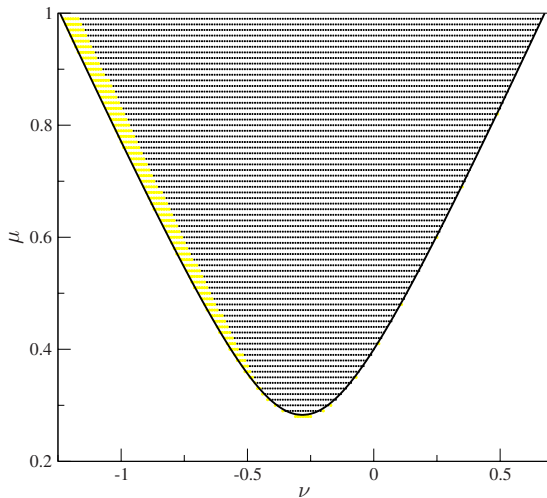


FIG. 2. (Color online) Simulation of a periodically forced ensemble [model Eq. (5) and (6)] with  $\beta = \text{const} = \pi/4$  and  $\varepsilon A(r, \varepsilon) = 1 - \varepsilon r^2$ , for  $\varepsilon = 1.4$ . For each point in the parameter plane  $\nu, \mu$  the simulation was performed twice, with nearly uniform and nearly identical initial conditions for oscillator phases. Black dots denote parameter values when both initial conditions lead to full synchrony; gray (yellow in color) dots denote the parameters when only nearly identical initial conditions lead to a fully synchronized state, while nearly uniform initial conditions lead to asynchrony. The border of the synchronization region nicely corresponds to the theoretical curve (black bold line), obtained according to Eq. (28).

**V. MEAN-FIELD LOCKING**

The case of full entrainment with  $r = 1$  is not the only possible stable dynamical regime in our system. In the other interesting regime the external force entrains only the mean field, while individual oscillators remain unsynchronized to forcing. We call this regime *mean-field locking* (MFL). First we illustrate it numerically and then provide a theoretical analysis.

**A. Illustration of the effect**

For the illustration of the effect of mean-field locking we solve numerically Eqs. (18) and (19) for the case of the non-

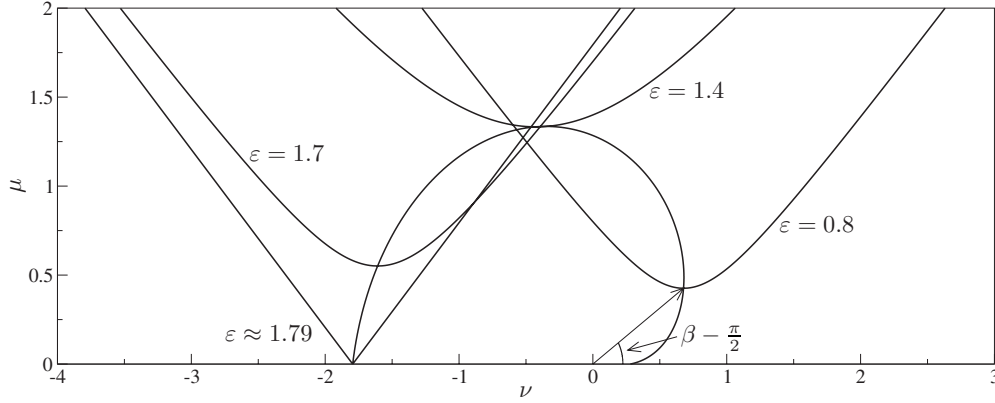


FIG. 3. Regions (tongues) of full synchrony for the harmonically forced ensemble with global nonlinear coupling [Eqs. (5) and (6)] with  $\beta = \beta_0 + \varepsilon^2 r^2$  and  $A=1$ . With variation in  $\varepsilon$  the tip of the tongue moves along a spiral. The tongues are plotted for  $\beta_0 = 0.475\pi$  and  $\varepsilon = 0.8$ ,  $\varepsilon = 1.4$ ,  $\varepsilon = 1.7$ , and  $\varepsilon = \sqrt{\pi + \varepsilon_q^2} \approx 1.79$ .

linearity in the amplitude function, i.e., we take  $\varepsilon A = 1 - \varepsilon r^2$ ,  $\varepsilon = 1.4$ , and  $\beta = 0$ . Note that for the chosen coupling strength, the critical value for the full synchrony is  $\mu_c = 0.4$  [see Eq. (27)]. First, we fix the amplitude of the external force at  $\mu = 0.2 < \mu_c$ , vary the forcing frequency  $\nu$ , and for each  $\nu$  compute  $\langle r \rangle$  and  $\langle \delta \rangle = \nu - \Omega$ , where  $\langle \cdot \rangle$  means time averaging. Then we repeat this numerical experiment for  $\mu = 0.6 > \mu_c$ . The results are shown in Fig. 5. We see that for  $\mu < \mu_c$  there exists a parameter range, where the mean-field frequency is locked to the external force. This locking increases the coherence of the ensemble; however, the force is not sufficiently strong in order to overcome the instability of the fully synchronous state due to the nonlinearity in the coupling. As a result, the amplitude of the mean field increases in the synchronization region, but remains less than unity.

In this figure we also plot the frequency of individual oscillators  $\omega_{osc}$ , computed according to Eq. (15), and see that in the MFL state the oscillators are not locked to the force (and, correspondingly, to the mean field). We remind that the

unforced system exhibits a bunch state, where the phases of the oscillators are scattered, but the frequencies of the oscillators and of the mean-field coincide. The forcing shifts both frequencies, but entrains only the frequency of the mean field  $\Omega$ . Thus, in this regime  $\omega_{osc}$  and  $\nu = \Omega$  become generally incommensurate, similarly to the SOQ state. For a stronger force,  $\mu > \mu_c$ , the mean-field amplitude reaches unity in the center of the synchronization region, so that both regimes of full synchrony and MFL are present; the borders of full synchrony correspond to Eq. (28). Finally, we note that a direct simulation of an ensemble of oscillators according to Eqs. (5) and (6) yields very similar results (not shown).

**B. Domain of mean-field locking**

The next step is to determine the domain of MFL regime from Eqs. (18) and (19). This can be done (semi)analytically for the case when in the MFL state  $r = \text{const}$  and  $\delta = \text{const}$ , what corresponds to the fixed point solution of Eqs. (18) and (19). (Another possible type of solution is discussed below.) Thus, we have:

$$0 = \varepsilon A(r, \varepsilon) r \cos \beta(r, \varepsilon) + \mu \cos \delta, \tag{30}$$

$$0 = \nu - \frac{1 + r^2}{2r} [\varepsilon A(r, \varepsilon) r \sin \beta(r, \varepsilon) + \mu \sin \delta]. \tag{31}$$

Excluding  $\delta$ , we obtain an equation for  $r$ :

$$[\varepsilon A(r, \varepsilon) r]^2 - \frac{4\nu r^2}{1 + r^2} \varepsilon A(r, \varepsilon) \sin \beta(r, \varepsilon) + \left( \frac{2\nu r}{1 + r^2} \right)^2 - \mu^2 = 0, \tag{32}$$

which we solve numerically for particular functions  $A$  and  $\beta$ . Picking up real valued solutions  $0 < r < 1$  and computing the eigenvalues of the found fixed point solutions  $r, \delta$  as described in Appendix A, we determine the existence domain of MFL regime for given  $\nu, \mu$  and the corresponding bifurcations.

We illustrate the determination of MFL domain by the same example as we used in Sec. IV ( $\varepsilon A = 1 - 1.4r^2$  and  $\beta = 0$ ) in Fig. 6. The first result is that, contrary to the case of

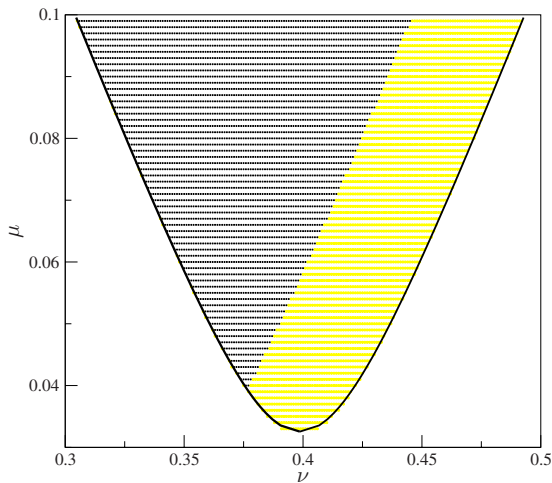


FIG. 4. (Color online) Simulation of a periodically forced ensemble Eqs. (5) and (6) with  $A(r, \varepsilon) = 1$  and  $\beta = \beta_0 + \varepsilon^2 r^2$ , for  $\beta_0 = 0.475\pi$  and  $\varepsilon = 0.4$ . Black bold curve is determined by Eq. (29). Gray (yellow in color) area corresponds to multistability (cf. Fig. 2).

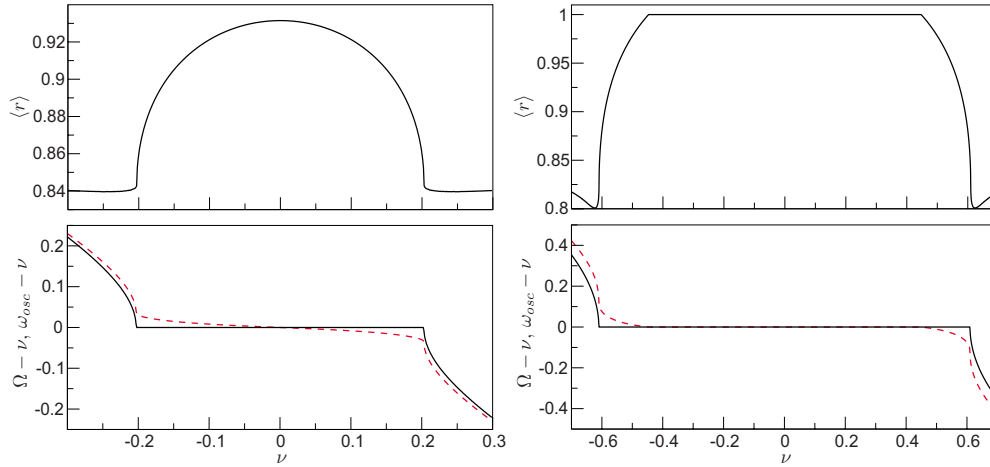


FIG. 5. (Color online) Illustration of the mean-field locking in a periodically driven oscillator ensemble with nonlinearity in the amplitude function (see text for details). Left column: subcritical driving  $\mu=0.2 < \mu_c$ . Right column: supercritical driving  $\mu=0.6 > \mu_c$ . In the lower plots red dashed and black solid lines show the frequencies of the individual oscillators and of the mean field, respectively. For  $\mu=0.2$  the force is not strong enough to induce full synchronization; it entrains the mean field, but not individual oscillators, so that  $r < 1$ . For  $\mu = 0.6$  there are both domains of full synchrony and of MFL. Nonlinearity in the amplitude function  $\varepsilon A(\varepsilon, r) = 1 - \varepsilon r^2$  and  $\beta = 0$ .

FS, the MFL has no threshold. For a small force, the loss of the MFL occurs via a saddle-node bifurcation, when one of the two real eigenvalues becomes positive. The lines of this bifurcation end in the vicinity of Takens-Bogdanov points, which can be found as discussed in Appendix B. Above these points, a desynchronization occurs via a Hopf bifurcation,

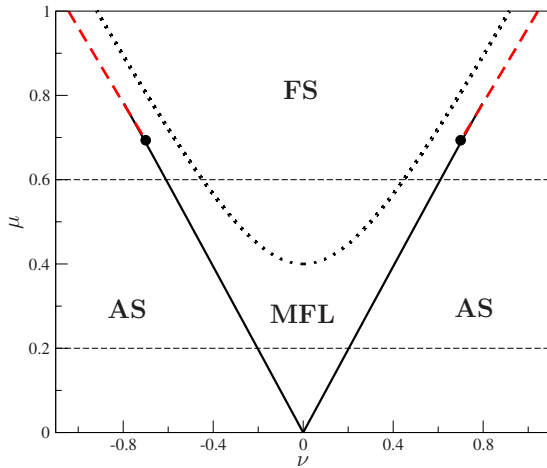


FIG. 6. (Color online) Bifurcation diagram for the forced ensemble with the amplitude nonlinearity (see text for details). Domains of FS, MFL, and asynchrony (AS) are seen. The black dotted curve is the border of the FS area, obtained via Eq. (28). Black solid and red dashed curves at the borders of the MFL domain correspond to the loss of synchrony via saddle-node and Hopf bifurcations, respectively. The black filled circles are codimension-2 Takens-Bogdanov points; the bifurcation structure in the vicinity of these points is shown in Fig. 11. Also, near Hopf bifurcation lines there exist narrow areas of MFL regimes with modulation in amplitude and phase (libration) which are not shown here (see text for details). The mean-field amplitude and frequencies of mean field and individual oscillators along the horizontal dashed lines are shown in Fig. 5. Nonlinearity in the amplitude function  $\varepsilon A(\varepsilon, r) = 1 - \varepsilon r^2$  and  $\beta = 0$ .

and here we have to distinguish two cases. First, the limit cycle that appears as a result of a Hopf bifurcation is small so that variation in  $\delta$  is less than  $2\pi$ , see Fig. 7. Expressed in the other way, the cycle in coordinates  $r \cos \delta, r \sin \delta$  does not revolve the origin. Physically, this means that the mean field is modulated both in the phase and the amplitude, but its frequency in average remains locked to the forcing; we denote such regimes as MFL with libration. The second case appears with the further variation in  $\nu$  when the limit cycle grows and the variation in  $\delta$  becomes unbounded. (The cycle in coordinates  $r \cos \delta, r \sin \delta$  now revolves the origin.) As a result, the mean-field locking is destroyed. (Note that the similar dynamics is known in the analysis of a forced weakly nonlinear oscillator [4], in a system of globally coupled stochastic phase oscillators [37], and in a forced Kuramoto model with the Lorentzian distribution [22].) In the immediate vicinity of the Takens-Bogdanov points complex bifurcations occur, see Appendix B.

Next, we briefly discuss what changes if  $\beta = \text{const} \neq 0$ ; this case is illustrated in Fig. 8. The main effect here is an appearance of bistability: there are domains where the asynchronous solution coexists with the MFL solution. On the right border this happens due to fact that the Hopf bifurcation here is subcritical; it means that the fixed point which corresponds to the MFL coexists with a stable limit cycle. The amplitude of the latter is large enough so that the MFL is immediately lost (no librations). In the bistability domain on the left border the fixed point solution (MFL) also coexists with a limit cycle; the latter, however, cannot be found from the stability analysis.

As the last example we consider the model with phase nonlinearity  $A = 1, \beta = \beta_0 + \varepsilon^2 r^2$ ; here we have taken  $\beta_0 = 0.475\pi$  and  $\varepsilon = 0.4$ . Qualitatively, the picture remains quite similar to the previous case of the model with amplitude nonlinearity [see Fig. 9 and compare with Figs. 6 and 8], just the synchronization regions becomes more asymmetric and the domains of multistability increase. Finally, we note that for all examples the results of a direct numerical simulation

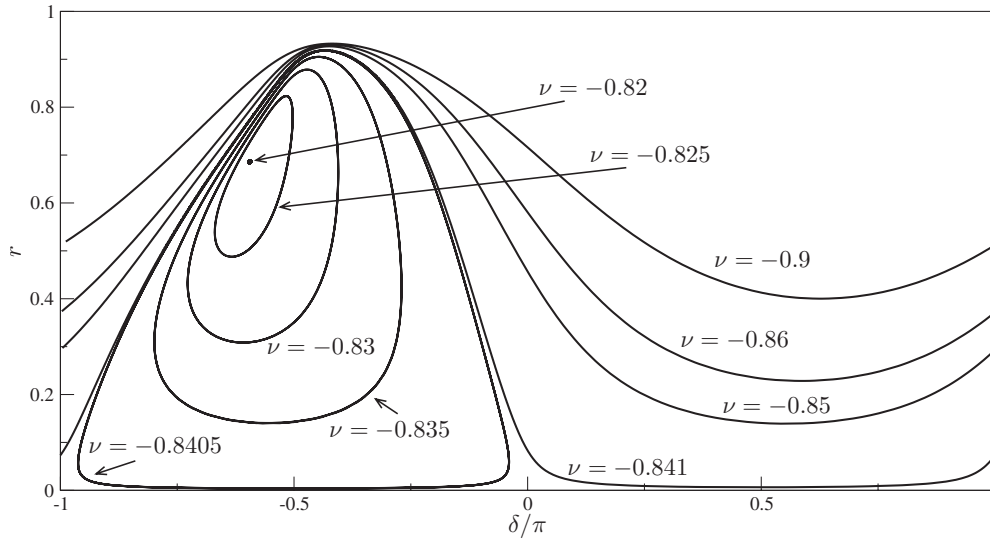


FIG. 7. Illustration of the desynchronization transition at large forcing (here  $\mu=0.8$ ). MFL corresponds to the fixed point (shown for  $\nu=-0.82$ ). With the decrease of forcing frequency  $\nu$  the limit cycle appears; however, first it is small and the deviation of phase difference  $\delta$  is bounded (libration). It means that on average the frequency of the mean field is still locked to the force. With further decrease in  $\nu$ , phase difference becomes unbounded (this takes place at  $\nu \approx -0.841$ ) and the synchrony gets lost. Nonlinearity in the amplitude function  $\varepsilon A(\varepsilon, r) = 1 - \varepsilon r^2$  and  $\beta = 0$ .

of an ensemble of 1000 oscillators are in a good correspondence with the analysis of Eqs. (18) and (19).

**C. Beyond the Ott-Antonsen manifold**

To conclude this section, we remind that Eqs. (18) and (19) have been derived under the assumption of uniformly distributed constants of motion  $\psi_k$ . This assumption means that the dynamics of the ensemble is confined to the reduced Ott-Antonsen manifold; as has been shown in [36], this

manifold is the only attractor if the oscillators are not identical but have a frequency distribution (and that is why this particular solution is especially important). The dynamics on this manifold is described by a simplified system of two Watanabe-Strogatz equations. However, for identical oscillators, generally one has to consider the full WS equation system, which generally possesses other solutions as well (see [30]). Moreover, the transients generally lie outside of the Ott-Antonsen manifold.

To illustrate this issue, we numerically analyze an ensemble of 1000 oscillators with nonlinearity in the amplitude function, and with a nonuniform distribution of constants of motion  $\psi_k$ . For this goal, we uniformly distribute one half of the constants  $\psi_k$  along the arc  $[(1-q)\frac{\pi}{2}, (1+q)\frac{\pi}{2}]$ , while the

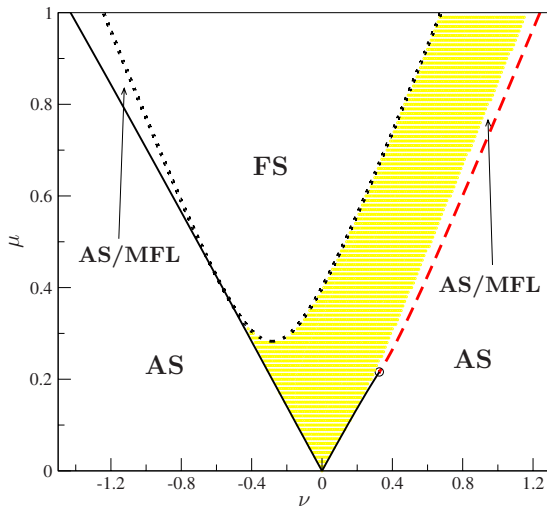


FIG. 8. (Color online) The same as in Fig. 6, but for  $\beta=0.25\pi$ . In addition to domains of FS, mean-field locking [gray (yellow) area], and AS, there are two domains where bistability MFL/AS is observed. Solid black and dashed red curves are lines of saddle node and Hopf bifurcations, respectively. Black circle shows the Takens-Bogdanov point (the second Takens-Bogdanov point lays outside of the shown range of  $\nu$  and  $\mu$ ).

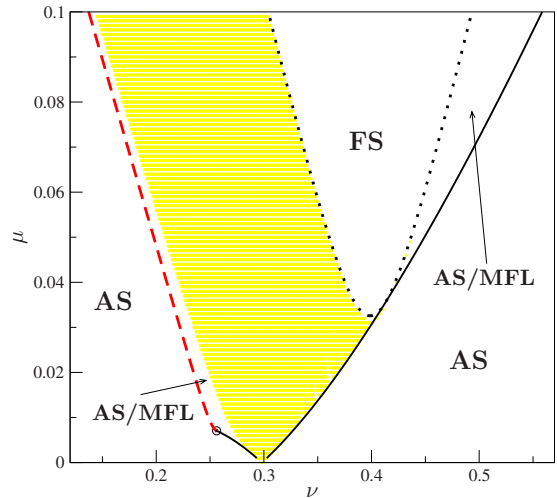


FIG. 9. (Color online) The same as in Figs. 6 and 8 but for the model with phase nonlinearity:  $A=1$ ,  $\beta = \beta_0 + \varepsilon^2 r^2$ , and  $\beta_0 = 0.475\pi$ .



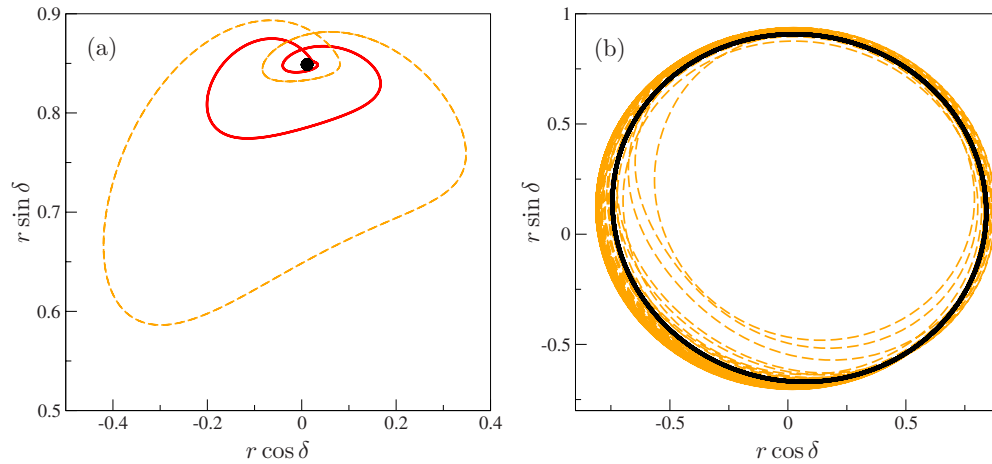


FIG. 10. (Color online) Simulation of the ensemble of  $N=1000$  oscillators with nonlinearity in the amplitude function and with different distribution of constants of motion; the distribution is parameterized by  $q$  (see text). Amplitude of the force is  $\mu=0.4$ . (a):  $\nu=0.4$ . Black circle, solid red, and orange dashed lines correspond to  $q=1$ ,  $q=0.9$ , and  $q=0.7$ , respectively. (b):  $\nu=0.6$ . Solid black and orange dashed lines correspond to  $q=1$  and  $q=0.7$ , respectively.

second half of the constants of motion is distributed along the arc  $[-(1+q)\frac{\pi}{2}, -(1-q)\frac{\pi}{2}]$ . Here  $0 \leq q \leq 1$  is a parameter; its largest value  $q=1$  corresponds to the uniform distribution of  $\psi_k$ , and, correspondingly, to the simplified theory presented above. Note that this choice of  $\psi_k$  satisfies constraints Eq. (11) and  $\sum \psi_k = 0$ . The initial values for the phases  $\phi_k$  are obtained with the help of Eq. (10), using the following initial values for the Watanabe-Strogatz variables:  $\Phi = \Psi = 0$ ,  $\rho = 0.05$ . The parameters of the system are  $\varepsilon = 1.4$ ,  $\mu = 0.4$ , and  $\beta = 0.25\pi$  (cf. Fig. 8), and the frequency of the forcing was varied. The result is as follows: in the middle of the synchronization region, e.g., for  $\nu=0.2$ , the value of parameter  $q$  does not influence the dynamics and we observe the MFL with a periodic mean field. Inside the synchronization region but close to its border, e.g., for  $\nu=0.4$ , the synchronized mean field becomes modulated both in the amplitude and the phase; in other words, we observe librations, see Fig. 10(a). Outside of the synchrony domain, e.g., for  $\nu=0.6$ , the dynamics of the mean field also contains a second frequency: we see that the torus is born from the limit cycle, see Fig. 10(b). We conclude that nonuniform distribution of constants of motion  $\psi_k$  generally leads to an appearance of an additional modulation, so that a static solution becomes periodic and a periodic solution becomes quasiperiodic.

## VI. DISCUSSION

We have analyzed the dynamics of periodically forced ensembles with global nonlinear coupling, for the case of identical phase oscillators. We have considered parameter values where the unforced ensemble exhibits partial synchrony, with the mean-field amplitude  $0 < r < 1$ . Depending on the type of the coupling nonlinearity, the oscillators in the autonomous ensemble either have the same frequency as the mean field, but different phases (bunch state), or the frequency of oscillators differs from that of the mean field and therefore the oscillators exhibit quasiperiodic dynamics.

It is natural to expect that a common external forcing increases the coherence in the system and tends to synchro-

nize all elements of the ensemble. However, the forcing has to overcome the instability of the synchronous solution due to the coupling nonlinearity. As a result, the state of full synchrony appears if the forcing amplitude exceeds some threshold value, even for identical oscillators. Next, there exists another synchronous state, which appears already for a very small forcing. In this state only the mean field of the population is locked to the external force, whereas the individual oscillators have a different, generally incommensurate frequency. The distribution of the phases has a hump which rotates with the same frequency as the force, and individual oscillators pass through this hump; the amplitude of the mean field is, respectively, between zero and one. If the parameters of the forcing are varied so that the system approaches the border of full synchrony, the distribution becomes more and more narrow, unless it collapses to a  $\delta$  function at the border of full synchrony. Thus, comparing synchronization properties of ensembles with linear and nonlinear coupling we conclude that nonlinearity results in a finite threshold of full synchrony. Furthermore, it leads to a synchronous state when the mean field of the oscillator is entrained, but individual oscillators are in a quasiperiodic state.

To conclude, there exist two levels of description of a forced ensemble. From the macroscopic viewpoint, the forced nonlinearly coupled ensemble behaves like a complex oscillator, which exhibits multistability at the borders of the synchronization region. The limit cycle of the collective mode is not very stable in the sense that a relatively weak force not only entrains the mode, but can also change its amplitude. The macroscopic description, based on the assumption of a uniform distribution of the constants of motion, leads to a low-dimensional system of equations and can be therefore fully analyzed. However, this macroscopic consideration is not sufficient for the detailed description of the mean-field dynamics: in dependence on the microscopic state of the ensemble, i.e., on the distribution of the constants of motion  $\psi_k$ , the collective mode dynamics may become quasiperiodic. Nevertheless, the macroscopic description yields

a correct (although “coarse grained”) picture of the main synchronization effects. Moreover, according to Ott and Antonsen [36], the solutions obtained from a macroscopic description are the only asymptotically stable solutions if oscillators have a continuous frequency distribution.

### ACKNOWLEDGMENTS

We gratefully acknowledge helpful discussions with G. Bordyugov and M. Zaks and financial support from DFG (SFB 555 and FOR 868).

### APPENDIX A: STABILITY ANALYSIS

For numerical analysis of Eqs. (18) and (19) it is convenient to present coordinates  $x=r \cos \delta$ ,  $y=r \sin \delta$  and rewrite the system as:

$$\begin{aligned} \dot{x} &= -\nu y + \frac{1-x^2-y^2}{2} \varepsilon A(x,y) x \cos \beta(x,y) + \frac{1+x^2+y^2}{2} \\ &\quad \times \varepsilon A(x,y) y \sin \beta(x,y) + \frac{\mu}{2} (1-x^2+y^2) = f(x,y), \\ \dot{y} &= \nu x - \frac{1+x^2+y^2}{2} \varepsilon A(x,y) x \sin \beta(x,y) + \frac{1-x^2-y^2}{2} \\ &\quad \times \varepsilon A(x,y) y \cos \beta(x,y) - \mu x y = g(x,y). \end{aligned}$$

In order to determine the stability of a fixed point solution, we compute the eigenvalues of the corresponding Jacobian matrix  $\lambda_{1,2} = (S \pm \sqrt{S^2 - 4J})/2$ , where

$$S = \frac{\partial f}{\partial x} + \frac{\partial g}{\partial y}, \quad J = \frac{\partial f}{\partial x} \frac{\partial g}{\partial y} - \frac{\partial f}{\partial y} \frac{\partial g}{\partial x}.$$

In the bunch state we have  $\varepsilon A(x,y) = 1 - \varepsilon(x^2 + y^2)$ ,  $|\beta(x,y)| = \text{const} \leq \pi/2$ . Presenting notation  $z = x^2 + y^2$ , we write the terms of the Jacobian as:

$$\begin{aligned} \frac{\partial f}{\partial x} &= -\varepsilon \left[ Ax^2 + \frac{z-1}{2} A + (1-z)x^2 \right] \cos \beta \\ &\quad + \varepsilon [Axy - (1+z)xy] \sin \beta - \mu x, \\ \frac{\partial f}{\partial y} &= -\nu - \varepsilon xy [A + (1-z)] \cos \beta \\ &\quad + \varepsilon \left[ Ay^2 + \frac{1+z}{2} A - (1+z)y^2 \right] \sin \beta + \mu y, \\ \frac{\partial g}{\partial x} &= \nu - \varepsilon \left[ Ax^2 + \frac{1+z}{2} A - (1+z)x^2 \right] \sin \beta \\ &\quad - \varepsilon xy [A + (1-z)] \cos \beta - \mu y, \\ \frac{\partial g}{\partial y} &= -\varepsilon xy [A - (1+z)] \sin \beta \\ &\quad - \varepsilon \left[ Ay^2 - \frac{1-z}{2} A + (1-z)y^2 \right] \cos \beta - \mu x. \end{aligned}$$

Next, we express  $x$  and  $y$  via  $z$  using Eqs. (30) and (31). Hence, all the terms of the Jacobian can be expressed via  $z$ . Substituting  $x(z)$  and  $y(z)$  in the above derivatives we obtain, after tedious but straightforward manipulations

$$S = 2a - bz, \quad (\text{A1})$$

$$J = a^2 + d^2 - (ab + dc)z, \quad (\text{A2})$$

where

$$a = \frac{1}{2}(1+z)(1-\varepsilon z) \cos \beta,$$

$$b = (1+\varepsilon - 2\varepsilon z) \cos \beta,$$

$$c = (1-\varepsilon - 2\varepsilon z) \sin \beta,$$

$$d = \frac{1-z}{1+z} \nu - \frac{1}{2}(1-\varepsilon z)(1-z) \sin \beta.$$

Thus, for given  $\nu$  and  $\mu$  we solve numerically Eq. (32), which for a given nonlinearity becomes an equation for  $z = r^2 \leq 1$ , and, substituting the solution in Eqs. (A1) and (A2), check its stability.

In the SOQ state we have  $A(x,y) = 1$ ,  $\beta(x,y) = \beta_0 + \varepsilon^2(x^2 + y^2) = \beta_0 + \varepsilon^2 z$ . Proceeding in the similar way as for the bunch state, we obtain the eigenvalues  $\lambda$  via  $z$ , using

$$S = 2a - cz,$$

$$J = a^2 + d^2 - (ac + bd)z,$$

where the functions  $a$ ,  $b$ ,  $c$ , and  $d$  now take the form

$$a = \frac{1+z}{2} \varepsilon \cos \beta(\varepsilon, z),$$

$$b = \varepsilon [\sin \beta(\varepsilon, z) + (1+z)\varepsilon^2 \cos \beta(\varepsilon, z)],$$

$$c = \varepsilon [\cos \beta(\varepsilon, z) + (1-z)\varepsilon^2 \sin \beta(\varepsilon, z)],$$

$$d = \frac{1-z}{1+z} \nu - \frac{\varepsilon}{2}(1-z) \sin \beta(\varepsilon, z).$$

### APPENDIX B: DYNAMICS IN THE VICINITY OF TAKENS-BOGDANOV POINTS

In the Takens-Bogdanov (TB) points both eigenvalues are zero, and, hence, in terms of variables introduced in Appendix A,  $S=0$  and  $J=0$ . Two latter equations can be solved to obtain these critical points. Let us begin with the bunch state case. Equation  $S=0$  becomes a quadratic equation, which root is:

$$z = z_c = 1 - \sqrt{1 - \frac{1}{\varepsilon}}. \quad (\text{B1})$$

(Here we took into account that  $0 \leq z \leq 1$  and  $\varepsilon > 1$ , so we dropped the second root). For given  $z_c$  the second equation,

$J=0$ , is a quadratic equation for  $d$ , its solution is

$$d_{1,2} = \frac{z_c}{2}(c \pm \sqrt{b^2 + c^2}),$$

where  $a$ ,  $b$ , and  $c$  are now computed for  $z=z_c$ . The expression for  $d$  can be now solved for  $\nu_c$ ; we obtain:

$$\nu_c = \frac{1+z_c}{1-z_c} \left( d_{1,2} + \frac{(1-\varepsilon z_c)(1-z_c)}{2} \sin \beta \right).$$

Finally, using Eqs. (30) and (31), we obtain

$$\mu_c = \sqrt{(1-\varepsilon z_c)^2 z_c + \frac{4\nu_c^2 z_c}{(1+z_c)^2} - \frac{4\nu_c z_c}{1+z_c} (1-\varepsilon z_c) \sin \beta},$$

what completes determination of Takens-Bogdanov points.

The same scheme can be used in the case of the SOQ state. However, instead of the quadratic Eq. (B1) we have a transcendental equation

$$\cot \beta(\varepsilon, z) = \varepsilon^2(1-z)z,$$

which should be solved numerically to yield  $z_c$ . Next steps are exactly the same as in the previous case and the final expressions are:

$$\nu_c = \frac{1+z_c}{1-z_c} \left( d_{1,2} + \frac{1-z_c}{2} \varepsilon \sin \beta(\varepsilon, z_c) \right),$$

$$\mu_c = \sqrt{\varepsilon^2 z_c + \frac{4\nu_c^2 z_c}{(1+z_c)^2} - \frac{4\nu_c z_c}{1+z_c} \varepsilon \sin \beta(\varepsilon, z_c)},$$

where

$$d_{1,2} = \frac{z_c}{2}(b \pm \sqrt{b^2 + c^2}).$$

We briefly illustrate the dynamics in the vicinity of TB points in Fig. 11, where we schematically present the bifurcation diagram near the left TB point; the bifurcation diagram for the right TB can be obtained by reflection with

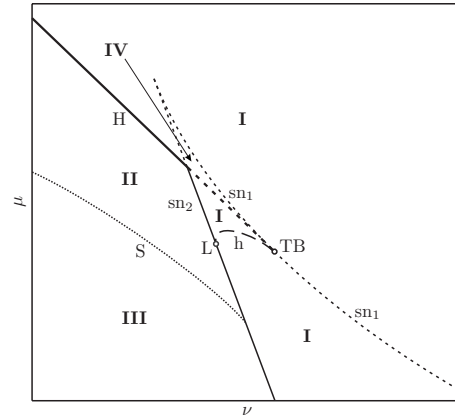


FIG. 11. Sketch of the bifurcation lines around the left TB point in Fig. 6. Here  $sn_1$  and  $sn_2$  are lines of the saddle-node bifurcation;  $H$  and  $h$  are lines of Hopf and homoclinic bifurcation, respectively; the line labeled by  $S$  marks the transition from librations to rotations. Domains I, II, and III correspond to fixed point solutions, librations, and rotations, respectively. In a very small domain IV we observe coexistence of two fixed point solutions, corresponding to two MFL states with different amplitudes of the mean field. The line  $sn_1$  (not shown in Fig. 6) goes from one TB point to the other and separates domains with one stable fixed point (beyond this line) and one stable and two unstable fixed points (below this line).

respect to the vertical axis. For computation of the bifurcation lines near TB points we used the AUTO 2000 package [38,39]. It is important to note that the diagram is qualitatively similar to diagrams given in Ref. [37], where Zaks *et al.* analyze dynamics of an ensemble of linearly coupled stochastic phase oscillators; therefore for details of bifurcations around TB points we refer to Ref. [37]. A similar bifurcation diagram also appeared in a recent publication [22], where Childs and Strogatz analyzed the dynamics of periodically forced Kuramoto model with Lorentzian distribution of natural frequencies.

- 
- [1] Y. Kuramoto, in *International Symposium on Mathematical Problems in Theoretical Physics*, Springer Lecture Notes Phys. Vol. 39 edited by H. Araki (Springer, New York, 1975), p. 420.
- [2] Y. Kuramoto, *Chemical Oscillations, Waves and Turbulence* (Springer, Berlin, 1984).
- [3] S. H. Strogatz, *Physica D* **143**, 1 (2000).
- [4] A. Pikovsky, M. Rosenblum, and J. Kurths, *Synchronization. A Universal Concept in Nonlinear Sciences* (Cambridge University Press, Cambridge, 2001).
- [5] E. Ott, *Chaos in Dynamical Systems*, 2nd ed. (Cambridge Univ. Press, Cambridge, 2002).
- [6] S. H. Strogatz, *Sync: The Emerging Science of Spontaneous Order* (Hyperion, New York, 2003).
- [7] J. A. Acebron, L. L. Bonilla, C. J. P. Vicente, F. Ritort, and R. Spigler, *Rev. Mod. Phys.* **77**, 137 (2005).
- [8] K. Wiesenfeld and J. W. Swift, *Phys. Rev. E* **51**, 1020 (1995).
- [9] A. F. Glova, *Quantum Electron.* **33**, 283 (2003).
- [10] I. Kiss, Y. Zhai, and J. Hudson, *Science* **296**, 1676 (2002).
- [11] D. Golomb, D. Hansel, and G. Mato, in *Neuro-informatics and Neural Modeling*, Handbook of Biological Physics Vol. 4 edited by F. Moss and S. Gielen (Elsevier, Amsterdam, 2001), pp. 887–968.
- [12] M. K. McClintock, *Nature (London)* **229**, 244 (1971).
- [13] Z. Néda, E. Ravasz, Y. Brechet, T. Vicsek, and A.-L. Barabási, *Nature (London)* **403**, 849 (2000).
- [14] S. H. Strogatz, D. M. Abrams, A. McRobie, B. Eckhardt, and E. Ott, *Nature (London)* **438**, 43 (2005).
- [15] L. Cimponeriu, M. G. Rosenblum, T. Fieseler, J. Dammers, M. Schiek, M. Majtanik, P. Morosan, A. Bezerianos, and P. A. Tass, *Prog. Theor. Phys.* **150**, (Suppl.), 22 (2003).
- [16] E. Montbrío, J. Kurths, and B. Blasius, *Phys. Rev. E* **70**, 056125 (2004).

- [17] J. H. Sheeba, V. K. Chandrasekar, A. Stefanovska, and P. V. E. McClintock, *Phys. Rev. E* **79**, 046210 (2009).
- [18] P. A. Tass, *Phase Resetting in Medicine and Biology. Stochastic Modelling and Data Analysis* (Springer-Verlag, Berlin, 1999).
- [19] Y. Kawamura, H. Nakao, K. Arai, H. Kori, and Y. Kuramoto, *Phys. Rev. Lett.* **101**, 024101 (2008).
- [20] T. W. Ko and G. B. Ermentrout, *Phys. Rev. E* **79**, 016211 (2009).
- [21] H. Sakaguchi, *Prog. Theor. Phys.* **79**, 39 (1988).
- [22] L. M. Childs and S. H. Strogatz, *Chaos* **18**, 043128 (2008).
- [23] E. Ott and T. M. Antonsen, *Chaos* **18**, 037113 (2008).
- [24] K. Okuda and Y. Kuramoto, *Prog. Theor. Phys.* **86**, 1159 (1991).
- [25] E. Barreto, B. Hunt, E. Ott, and P. So, *Phys. Rev. E* **77**, 036107 (2008).
- [26] M. G. Rosenblum and A. S. Pikovsky, *Phys. Rev. Lett.* **92**, 114102 (2004).
- [27] M. G. Rosenblum and A. S. Pikovsky, *Phys. Rev. E* **70**, 041904 (2004).
- [28] D. M. Abrams, R. Mirollo, S. H. Strogatz, and D. A. Wiley, *Phys. Rev. Lett.* **101**, 084103 (2008).
- [29] M. G. Rosenblum and A. S. Pikovsky, *Phys. Rev. Lett.* **98**, 064101 (2007).
- [30] A. S. Pikovsky and M. G. Rosenblum, *Physica D* **238**, 27 (2009).
- [31] H. Sakaguchi and Y. Kuramoto, *Prog. Theor. Phys.* **76**, 576 (1986).
- [32] S. Watanabe and S. H. Strogatz, *Phys. Rev. Lett.* **70**, 2391 (1993).
- [33] S. Watanabe and S. H. Strogatz, *Physica D* **74**, 197 (1994).
- [34] A. S. Pikovsky and M. G. Rosenblum, *Phys. Rev. Lett.* **101**, 264103 (2008).
- [35] S. A. Marvel, R. E. Mirollo, and S. H. Strogatz, e-print arXiv:0904.1680.
- [36] E. Ott and T. M. Antonsen, *Chaos* **19**, 023117 (2009).
- [37] M. A. Zaks, A. B. Neiman, S. Feistel, and L. Schimansky-Geier, *Phys. Rev. E* **68**, 066206 (2003).
- [38] A. R. Champneys, Yu. A. Kuznetsov, and B. Sandstede, *Int. J. Bifurcat. Chaos* **6**, 867 (1996).
- [39] E. J. Doedel, R. C. Paffenroth, A. R. Champneys, T. F. Fairgrieve, Y. A. Kuznetsov, B. Sandstede, and X. Wang, *Tech. Rep* (Caltech, Pasadena, 2001).
- [40] We use variables, related to the original WS variables  $\tilde{\rho}$ ,  $\tilde{\Psi}$ , and  $\tilde{\Phi}$  as  $\tilde{\rho} = \frac{2\rho}{1+\rho^2}$ ,  $\tilde{\Psi} + \pi = \Psi$ ,  $\tilde{\Phi} + \pi = \Phi$ .
- [41] Nearly uniform initial conditions means that phases are taken uniformly from 0 to  $2\pi$  and then one phase is shifted by 0.001. Nearly identical initial conditions mean that the phases  $\phi_k$  are uniformly distributed on an arc  $0.0005\pi$ .